Preparation, Functional Characterization, and NMR Studies of Human KCNE1, a Voltage-Gated Potassium Channel Accessory Subunit Associated with Deafness and Long QT Syndrome[†,‡]

Changlin Tian,[§,||] Carlos G. Vanoye,[⊥] Congbao Kang,[§] Richard C. Welch,[⊥] Hak Jun Kim,[§] Alfred L. George, Jr.,[⊥,▽] and Charles R. Sanders*[,§]

Department of Biochemistry, Center for Structural Biology, Department of Medicine, and Department of Pharmacology, Vanderbilt University School of Medicine, Nashville, Tennessee 37232-8725

Received April 14, 2007; Revised Manuscript Received July 25, 2007

ABSTRACT: KCNE1, also known as minK, is a member of the KCNE family of membrane proteins that modulate the function of KCNQ1 and certain other voltage-gated potassium channels (K_V). Mutations in human KCNE1 cause congenital deafness and congenital long QT syndrome, an inherited predisposition to potentially life-threatening cardiac arrhythmias. Although its modulation of KCNQ1 function has been extensively characterized, many questions remain regarding KCNE1's structure and location within the channel complex. In this study, KCNE1 was overexpressed in *Escherichia coli* and purified. Micellar solutions of the protein were then microinjected into *Xenopus* oocytes expressing KCNQ1 channels, followed by electrophysiological recordings aimed at testing whether recombinant KCNE1 can co-assemble with the channel. Nativelike modulation of channel properties was observed following injection of KCNE1 in lyso-myristoylphosphatidylglycerol (LMPG) micelles, indicating that KCNE1 is not irreversibly misfolded and that LMPG is able to act as a vehicle for delivering membrane proteins into the membranes of viable cells. $^{1}H-^{15}N$ TROSY NMR experiments indicated that LMPG micelles are well-suited for structural studies of KCNE1, leading to assignment of its backbone resonances and to relaxation studies. The chemical shift data confirmed that KCNE1's secondary structure includes several α-helices and demonstrated that its distal C-terminus is disordered. Surprisingly, for KCNE1 in LMPG micelles, there appears to be a break in α-helicity at sites 59−61, near the middle of the transmembrane segment, a feature that is accompanied by increased local backbone mobility. Given that this segment overlaps with sites 57−59, which are known to play a critical role in modulating KCNQ1 channel activation kinetics, this unusual structural feature likely has considerable functional relevance.

Voltage-gated potassium channels (K_V)[1] play a variety of important roles in human health and disease. For example, human KCNQ1 is essential to the cardiac action potential that mediates heartbeat and is also critical for potassium ion homeostasis in the inner ear (*1*, *2*). The function of several K_V channels is modulated by accessory proteins, including K_V channel β subunits ($K_V\beta$) (*3*−*6*), potassium channel interacting proteins (KCHiPs) (*7*, *8*), and the KCNE family of single-transmembrane proteins, including KCNE1 and minK-related peptides (MiRPs) (*9*−*14*). KCNE1, also known as minK, co-assembles with KCNQ1 in heart muscle cells to form a channel complex that generates the slowly activating cardiac potassium current (I_{Ks}), an important determinant of myocardial repolarization (*9*, *12*, *14*). KCNE1 alters several biophysical properties of KCNQ1 channels. The fully activated whole-cell current is 4−6 times larger when KCNQ1 is complexed with KCNE1; the channel activation rate is reduced by more than 1 order of magnitude, and activation occurs at more positive potentials (*9*−*14*). The importance of KCNE1 in regulating KCNQ1 channel func-

[†] This study was supported by NIH Grant R01 DC007416 to C.R.S., NIH Grant HL077188 to A.L.G., a Vanderbilt School of Medicine Discovery Grant to C.G.V., and a postdoctoral fellowship from the American Heart Association to C.T. (0625586B). Some data were collected in the SEC NMR facility at the University of Georgia, which is supported by U.S. NIH Grant P41 GM066340.

[‡] The NMR assignments for KCNE1 that are reported in this paper have been deposited in the BMRB as entry 15102.

* To whom correspondence should be addressed. E-mail: chuck.sanders@vanderbilt.edu. Phone: (615) 936-3756. Fax: (615) 936-2211.

[§] Department of Biochemistry and Center for Structural Biology.

[||] Current address: School of Life Science, University of Science and Technology of China, Hefei, Anhui 230026, People's Republic of China.

[⊥] Department of Medicine.

[▽] Department of Pharmacology.

[1] Abbreviations: BME, β-mercaptoethanol; CMC, critical micelle concentration; DDM, β-dodecyl maltoside; DM, β-decyl maltoside; DPC, dodecylphosphocholine; DSS, 2,2-dimethyl-2-silapentane-5-sulfonate; DTAB, dodecyltrimethylammonium bromide; IPTG, isopropyl thiogalactoside; K_V, voltage-gated potassium channel; LMPC, lysomyristoylphosphatidylcholine; LMPG, lysomyristoylphosphatidylglycerol; NMR, nuclear magnetic resonance; NOE, nuclear Overhauser effect; OD_{280}, optical density at 280 nm for a sample with a path length of 1 cm; OG, β-octyl glucoside; PMAL-C12, zwitterionic amphipathic polymer prepared by stoichiometric substitution (amidation with carboxylate generation) of the anhydride groups in poly(maleic anhydride-alt-1-tetradecene) with 3-(dimethylamino)propylamine; QT interval, phenomenological parameter that is extracted from electrocardiogram recordings that are used to monitor cardiac function in clinical settings; SDS, sodium dodecyl sulfate; T_1, longitudinal NMR relaxation time; T_2, transverse NMR relaxation time; TM, transmembrane; TROSY, transverse relaxation optimized spectroscopy.

10.1021/bi700705j CCC: $37.00
Published on Web 09/25/2007

tion is reflected by the fact that a number of inherited mutations in KCNE1 result in long QT syndrome (*15*−*18*) and deafness (*19*). Other members of the KCNE family can also modulate KCNQ1 function, each in an electrophysiologically distinct manner (*9*, *12*, *14*, *20*). For example, KCNE3 expression increases the magnitude of KCNQ1-mediated currents without slowing channel activation (*21*). Moreover, KCNE family members have been shown to modulate other K_V channels in addition to KCNQ1 (*9*, *10*, *12*, *14*, *19*, *20*, *22*, *23*).

Much is known about the structural basis for K_V channel function thanks to the combined efforts of structural biology and decades of structure−function electrophysiological studies. However, much less is known regarding the structural biophysical basis for the regulation of KCNQ1 and other K_V channels by the KCNE family of accessory subunits. Biochemical, mutagenesis, and electrophysiological studies have led to predictions of proximity between certain sites in KCNE1 and KCNQ1 (*13*, *24*−*30*). Accompanying these studies has been a lively debate regarding whether KCNE1 is actually located in the ion conduction pathway or instead modulates function by interacting with the outer (membrane-disposed) regions of the channel domain. Direct structural biophysical studies of interactions of KCNE1 with K_V channels have not yet been reported. Indeed, while there have been a number of NMR and other biophysical studies of polypeptide fragments of KCNE1 (*31*−*35*), structural studies of the intact protein have not yet been reported. We have therefore initiated NMR structural studies of full-length KCNE1 in model membranes (i.e., detergent micelles). The first stage of this work entailed bacterial expression of KCNE1 followed by purification.

Escherichia coli has previously been used to overexpress many integral membrane proteins, including a number of ion channels, for use in biochemical and structural studies. Advantages of this approach include rapid cell growth, inexpensive media, capacity for uniform isotopic labeling, and the availability of divers cloning vectors. However, few human membrane proteins have been overexpressed in bacteria, and even fewer have subsequently been shown to retain functionality. Moreover, while some classes of membrane proteins have functions that can readily be tested, this is very challenging for channel accessory subunits such as KCNE1, which lack intrinsic assayable functions. This problem is exacerbated when the experiments of interest will be carried out using detergent micelles as the model membrane medium. Micelles have been very commonly used to mimic the lipid membrane environment of membrane proteins in structural and functional studies but cannot be employed in assays of channel function because of the lack of inside−outside aqueous compartmentalization in micelles. Moreover, not all detergents can maintain the native folded structure of any given membrane protein.

In this study, we developed a high-level *E. coli*-based overexpression system for human KCNE1 and purified the protein in a variety of types of micelles. To assess the degree to which the recombinant protein maintains a nativelike structural state in the detergent solutions, aliquots were microinjected into *Xenopus* oocytes expressing human KCNQ1 channels to test whether the reconstituted KCNE1 can associate with and modulate the channels. Micellar systems that successfully sustained KCNE1 function were then tested for their potential as a medium for NMR-based structural studies. One detergent, LMPG, was found to be superior both at sustaining KCNE1 function and as a medium from which high-quality solution NMR spectra of the protein can be obtained. NMR-based assessment of KCNE1's secondary structure and dynamics in LMPG micelles also provided results that were both surprising and, when correlated with structure−function data available for KCNE1 modulation of the KCNQ1 channel, intriguing.

MATERIALS AND METHODS

Cloning and Overexpression of Human KCNE1. The cDNA for human KCNE1 was cloned into expression vector pET16b (Novagen Inc., La Jolla, CA) using the Seamless cloning approach (Stratagene, La Jolla, CA), which was based on use of polymerase chain reaction (PCR) with the *Eam1104I* enzyme only (*36*). Primers containing *Eam1104I* sites were used to amplify both the inserted KCNE1 gene and the pET16b vector, which provided directional cloning during subsequent ligation reactions. In the final construction, the Factor Xa protease cleavage site and associated spacer were removed during cloning and the full-length KCNE1 gene was positioned immediately after a hexahistidine tag (His_6) followed by a single glycine (Figure 1A). The construct was verified by sequencing.

Expression of the His_6-tagged KCNE1 protein in the pET16b vector was under the control of an IPTG-inducible promoter. The expression construction was transformed into *E. coli* BL21(DE3) CodonPlus-RP cells (Stratagene). Successful transformants were grown in M9 minimal medium with 100 μg/mL ampicillin and 34 μg/mL chloramphenicol and supplemented with a multivitamin (CVS Spectravite, $^1/_{10}$ tablet/L of medium). The culture was incubated at 37 °C and 225 rpm, until the OD_{600} reached 0.9, at which point protein expression was induced using 1 mM IPTG, followed by continued rotary shaking at 37 °C for 8 h.

Purification of KCNE1 in Detergent Micelles. Cells expressing recombinant KCNE1 were harvested by centrifugation at 4 °C and then suspended in 20 mL of lysis buffer [70 mM Tris-HCl and 300 mM NaCl (pH 8.0)] per gram of wet cells, with 2 mM β-mercaptoethanol (BME). The cell suspension was probe-sonicated (F550 sonic dismembrator, Misonix, Farmingdale, NY; power level of 6.0, 5 s pulses separated by 5 s) for 5 min on ice. The lysates were twice passed through an EmulsiFlex C3 high-pressure homogenizer (Avestin, Ottawa, ON). Magnesium acetate (to 5 mM), DNase (to 0.02 mg/mL), and RNase (to 0.02 mg/mL) were then added, and the lysate was rotated at 4 °C for 2 h. The lysate was centrifuged at 4 °C and 40000*g* for 20 min. The supernatant was discarded, and the inclusion body pellet was washed twice and centrifuged twice using the same lysis buffer.

Inclusion bodies were suspended in binding buffer [20 mM Tris, 100 mM NaCl (pH 7.0), 8 M urea, and 0.2% (w/v) SDS] and rotated at room temperature for 2 h to dissolve the inclusion bodies, followed by centrifugation at room temperature and 40000*g* for 20 min to remove insoluble cell debris. The supernatant containing solubilized KCNE1 was incubated with 5 mL of Ni(II)-NTA chromatographic resin (Superflow, Qiagen, Valencia, CA) per liter of original culture, which was rotated at room temperature for at least

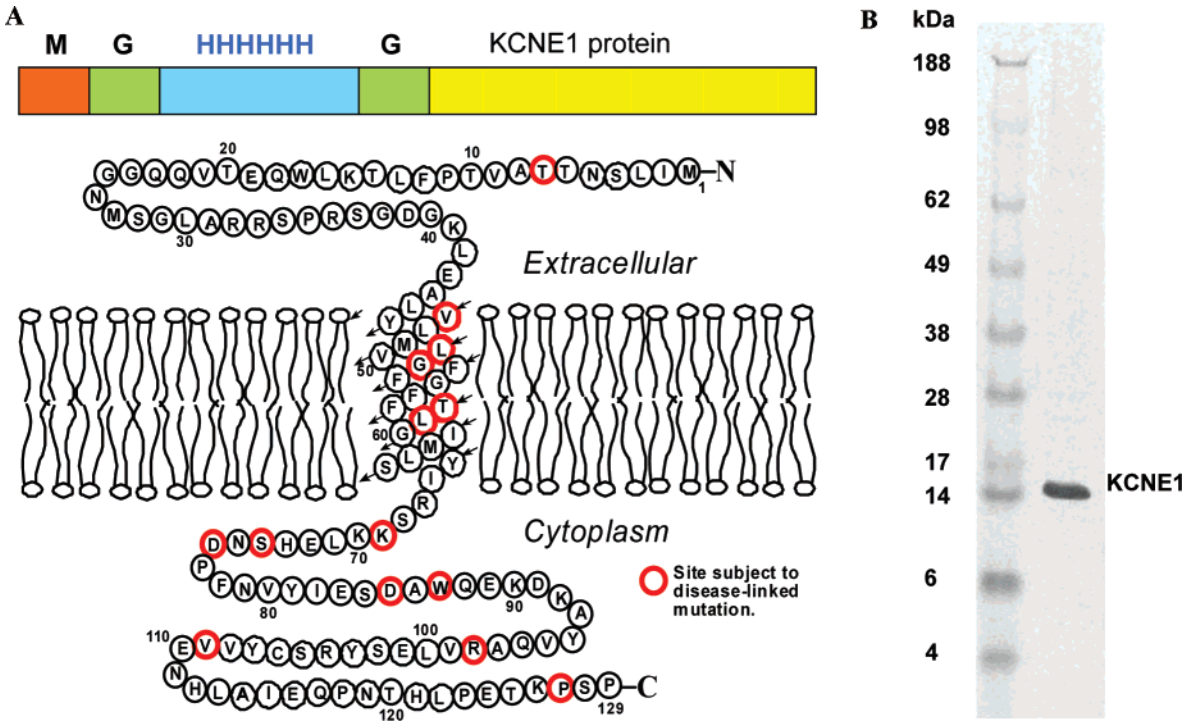

FIGURE 1: (A) Construction of tagged KCNE1 that was used in this study (top) and sequence and predicted membrane topology of full-length untagged wild-type human KCNE1 (GenBank accession number L28168) (bottom). The small arrows shown for the TM segment show the tracing of the peptide chain. Nothing is implied by this panel with regard to the conformation of the protein. (B) SDS−PAGE with Coomassie staining following expression and purification of His_6-KCNE1 into LMPG micelles. The mobility of His_6-KCNE1 in the SDS−PAGE gel is compatible with its molecular mass (15.7 kDa). The identity of this band as tagged KCNE1 was confirmed by mass spectrometry.

30 min. The resin was then packed into a gravity-flow column and washed with 8 bed volumes of binding buffer. Impurities were eluted using a wash buffer [20 mM Tris-HCl, 100 mM NaCl (pH 7.0), and 0.2% SDS, without urea] until the OD_{280} returned to baseline. To exchange the detergent from SDS to a nondenaturing detergent, 10 column volumes of rinse buffer [20 mM Tris-HCl and 100 mM NaCl (pH 7.0)] containing one detergent, 0.5% OG, 0.5% DM, 0.5% DDM, 0.5% DPC, 0.2% DPC/SDS (10:1), 0.5% DPC/SDS (10:1), PMAL-C12, 0.2% DTAB, 0.2% LMPC/LMPG (4:1), or 0.2% LMPG, was used to re-equilibrate the column. KCNE1 was then eluted using a buffer containing the same detergent with 250 mM imidazole (analytical grade) (pH 6.0). The pH of the solution after elution was tested and, if required, readjusted to 6.0 using acetic acid. All chromatographic buffers contained 2 mM BME. The concentration of the purified protein was determined from the OD_{280} using an extinction coefficient of 1.2 mg/mL protein per OD_{280} unit in a 1 cm cell. The protein was confirmed as KCNE1 using proteolytic digestion and MALDI-based tandem mass spectrometry (MS/MS) in the Vanderbilt Proteomics Core.

Electrophysiological Functional Analysis of KCNQ1 and KCNE1. cDNAs for KCNQ1 and KCNE1 were constructed in plasmid vectors pSP64T and pRc/CMV, respectively, as previously described (*29*). cRNA was then transcribed in vitro from *Eco*RI-digested (pSP64T-KCNQ1) or *Xba*I-digested (pRc/CMV-KCNE1) linear cDNA templates using Sp6 or T7 RNA polymerase and the mMessage mMachine transcription system (Ambion Inc., Austin, TX). The size and integrity of cRNA preparations were evaluated by formaldehyde−agarose gel electrophoresis, and full-length cRNA concentrations were estimated by comparison with a 0.24−9.5 kb RNA ladder (Sigma, St. Louis, MO).

Female *Xenopus laevis* were anesthetized by immersion in 0.2% tricaine for 15−30 min. Ovarian lobes were removed, and oocytes were manually defolliculated. Stage V−VI oocytes were injected with 25 nL of cRNA (KCNQ1, 6 ng/oocyte; KCNE1 constructs, 3 ng/oocyte) and incubated at 18 °C for 48−72 h in L-15 (Leibovitz's medium, Invitrogen) diluted 1:1 with water and supplemented with penicillin (150 μg/mL) and streptomycin (150 μg/mL). Some oocytes were injected with 25 nL of water as controls for endogenous currents. Because previous studies revealed that *Xenopus* oocytes express an endogenous KCNE family gene (*37*), control currents from oocytes injected with only KCNQ1 cRNA were always recorded from each batch to test for possible channel modulation by endogenous KCNE subunits.

Currents were recorded at room temperature 2−3 days after injection using a two-microelectrode voltage-clamp technique with an OC-725B amplifier (Warner Instruments Corp., Hamden, CT). Oocytes were bathed at room temperature (22−25 °C) in a modified ND96 solution containing 96 mM NaCl, 4 mM KCl, 2 mM $MgCl_2$, 0.1 mM $CaCl_2$, and 5 mM HEPES (pH 7.6, ~200 mosmol/kg). Data were recorded using Clampex 7 (Molecular Devices Corp., Sunnyvale, CA), filtered at 500 Hz, and digitized at 2 kHz. Data were analyzed and plotted using a combination of Clampex, SigmaPlot 2000 (SPSS Science, Chicago, IL), and Origin 7.0 (OriginLab, Northampton, MA). Current−voltage and normalized isochronal voltage−activation relationships were obtained by measuring current for 2 s during depolar-

izing pulses between −50 and 60 mV from a holding potential of −80 mV. The normalized isochronal data were fit with a Boltzmann function of the form $1/\{1 + \exp[(V - V_{1/2})/k_v]\}$, where $V_{1/2}$ is the half-maximal activation voltage and k_v is the slope factor. Oocytes with currents at −80 mV (holding potential) larger than currents measured for water-injected oocytes (−0.15 μA) were considered leaky and not used for analysis.

Injection of Micellar Solutions of His_6-KCNE1 into Xenopus Oocytes and Electrophysiological Functional Analysis. Functional analysis was performed as described above with the exception that oocytes were first injected with cRNA encoding KCNQ1 (25 nL, 6 ng/oocyte). This was followed 24 h later by injection of 25 nL of 0.8 mg/mL His_6-KCNE1 protein or protein-free detergent micelles. Whole-cell currents were measured 24 h after injection of micellar solutions. An average oocyte volume is 700 nL (1.0−1.2 mm diameter). With injections of 25 nL, all detergent solutions tested in this work were diluted to well below their nominal critical micelle concentrations. For example, the nearly 30-fold dilution of a 0.1% LMPG solution leads to a final concentration of 75 μM, well below its reported critical micelle concentration of 0.2−0.3 mM (*38*). It should also be noted that microinjection often transiently ruptures oocytes, which typically reseal to remain viable. Only viable oocytes were used for electrophysiological measurements.

All experimental conditions were tested using oocytes from at least three frogs. Data are represented as means ± the standard error, and in some figures, error bars are smaller than the symbols. The numbers of experiments (oocytes) are provided in the figure legends.

Sample Preparation and Two-Dimensional NMR Spectroscopy of KCNE1. Purified [U-^{15}N]His_6-KCNE1 was prepared in one of following micellar solutions: 300 mM DPC, 300 mM DPC/SDS (molar ratio of 10:1), 300 mM SDS, 150 mM LMPC/LMPG (molar ratio of 4:1), 300 mM DPC, or 150 mM LMPG. The 10:1 DPS/SDS and 4:1 LMPC/LMPG solutions were included because they represent zwitterionic/anionic detergent mixtures that mimic the ca. 10−20 mol % anionic lipid composition of typical biological membranes.

To the eluted protein solution were added EDTA and DTT to final concentrations of 2 mM, and D_2O was added to a final concentration of 10% (v/v). The pH was adjusted to pH 6.0 using acetic acid and then concentrated to a volume of 500 μL using an Amicon Ultra-15 centrifugal filter device (10 kDa cutoff; Millipore, Bedford, MA). Samples were then transferred to 5 mm NMR tubes. The KCNE1 concentration was usually adjusted to 1.0 mM. KCNE1 had a tendency to form visible aggregates over a time scale of days upon incubation at higher concentrations and at temperatures above room temperature. Solutions of 1 mM KCNE1 in LMPG detergent micelles can be safely stored at 4 °C for ∼1−2 months. For longer-term storage, samples were frozen in liquid nitrogen and then stored in a −80 °C freezer.

Two-dimensional ^{1}H−^{15}N correlation spectra of KCNE1 in different detergent micelles were recorded at 40 °C using the Weigelt version of the TROSY pulse sequence (*39*) on a 600 MHz Bruker (Billerica, MA) spectrometer. 256 and 1024 complex points were acquired in the t_1 time domain (^{15}N dimension) and t_2 time domain (^{1}H dimension), respectively. The data were zero-filled to 512 × 2048 and apodized using a Gaussian window function prior to Fourier transformation using NMRPipe (*40*).

Assignment of KCNE1's Backbone NMR Resonances. Uniformly ^{2}H-, ^{13}C-, and ^{15}N-labeled KCNE1 was prepared in LMPG micelles with 1.0 mM protein and 4% detergent in a buffer containing 250 mM imidazole, 2 mM EDTA, 2 mM DTT, and 10% D_2O (pH 6.0). NMR data were collected at 40 °C on either a Varian Inova 900 MHz spectrometer with a cryoprobe or a Bruker Avance 600 MHz spectrometer using a conventional probe. Proton chemical shifts were referenced to internal DSS, and ^{13}C and ^{15}N chemical shifts were referenced indirectly to DSS using absolute frequency ratios. The following series of three-dimensional (3D) experiments were used for sequential resonance assignments: TROSY-HNCO, TROSY-HNCA, TROSY-HN(CO)CA, TROSY-HNCACB, and TROSY-HN-(CO)CACB (*41*). To aid assignments, KCNE1 was also prepared in M9 medium that was supplemented with specific ^{15}N-labeled amino acids (300 mg/L Tyr, 150 mg/L Phe, 300 mg/L Ile, 300 mg/L Leu, 300 mg/L Val, 150 mg/mL Met, or 150 mg/L Cys) and an excess of all other amino acids in unlabeled form. The ensuing amino acid type-specific two-dimensional (2D) ^{1}H−^{15}N TROSY spectra were invaluable for resolving ambiguities in the preliminary resonance assignments that arose both from the modest spectral dispersion and from the relatively broad resonance line widths observed for most peaks. Spectra were processed using NMRPipe (*40*) and analyzed using NMRView (*42*).

Attempts to assign KCNE1's side chain resonances using TOCSY-based NMR pulse sequences were not successful because of the unfavorable relaxation properties for the side chain resonances as a consequence of the relatively large size (estimated to be 60 kDa) of the KCNE1−LMPG micellar complex. It is very possible that KCNE1 is a suitable candidate for application of "methyl-TROSY" labeling and related pulse sequence technology (*43*) for selectively assigning the side chain methyl groups of Ile, Val, and Leu residues, but this has not yet been undertaken.

NMR Relaxation Experiments. Uniformly ^{2}H- and ^{15}N-labeled KCNE1 was prepared at a concentration of 0.4 mM in a buffer containing 250 mM imidazole (pH 6.0), 2 mM DTT, 2 mM EDTA, and 10% D_2O. TROSY-based 2D pulse sequences were used for determination of T_1, T_2, and ^{1}H−^{15}N steady-state NOEs (*44*). The relaxation experiments were performed at 600 and 800 MHz and at 313 K. T_1 values were determined from a series of ^{1}H−^{15}N correlation spectra with 100, 200, 400, 800, 1200, 1600, 2000, and 2400 ms relaxation evolution delays. The T_2 values were obtained from the spectra with 6, 18, 30, 54, 78, 114, 150, and 198 ms delays. The steady-state ^{1}H−^{15}N NOE values were determined from peak ratios observed between two spectra, one collected with a 3 s presaturation of protons and the other without proton presaturation. The spectra were processed using NMRPipe and analyzed with NMRView.

RESULTS

Expression and Purification of Human KCNE1. His_6-KCNE1 was overexpressed with an N-terminal purification tag (Figure 1A) into inclusion bodies using a strain of *E. coli* optimized for translation of mRNA containing rare codons. That His_6-KCNE1 expressed in inclusion bodies in

E. coli is not surprising given that mammalian membrane proteins often are not incorporated well into the plasma membrane of *E. coli*. Moreover, the fact that KCNE1's transmembrane domain is bounded on both ends by several positively charged residues in both juxtamembrane segments dictates that insertion of this protein into the plasma membrane by the cellular insertion apparatus would not be expected because this would violate the "positive inside rule" that characterizes the topology of juxtamembrane Lys and Arg residues observed for most native membrane proteins of *E. coli* and many other organisms (*45*).

A flexible protocol was developed to purify KCNE1 into detergent micelles using Ni(II)-NTA-based metal ion chelate chromatography. Inclusion bodies were solubilized using 8 M urea and a harsh detergent, SDS, followed by binding to Ni(II) metal ion affinity resin and elution of all impurities. On-resin refolding of KCNE1 was accomplished by re-equilibrating the column with a nondenaturing detergent solution (e.g., DDM or LMPG), followed by elution of pure protein in micelles of the same detergent. The yield of KCNE1 was observed to vary with the detergent employed at the final stages of purification, although the final protein was always observed to be of high purity (cf., Figure 1B). Yields of pure protein (milligrams of pure KCNE1 per liter of culture) were $\ll$1 (OG or DM), $<$1 (DDM), 1 (DTAB or PMAL-C12), 2 (DPC), 7 (4:1 LMPC/LMPG), and 10 (SDS or LMPG). The different elution yields reflect the dependence of KCNE1 solubility on micellar environment, with anionic micelles clearly being preferred by KCNE1 over neutral detergents (OG, DM, and DDM), zwitterionic detergents (DPC and LMPC), cationic detergents (DTAB), or zwitterionic amphipathic polymers, "amphipols" (PMAL-12). Cross-linking of purified KCNE1 in these mixtures using 20 mM glutaraldehyde, followed by SDS−PAGE, indicated that KCNE1 in each of the three neutral detergents is highly prone to form high-molecular weight aggregates, an observation that may explain the low purification yields observed for these detergents. These neutral detergent/KCNE1 mixtures were not subjected to further characterization in this work.

Functional Expression of Human His$_6$-KCNE1 in Xenopus Oocytes. To test whether the His$_6$ tag interferes with KCNE1 native function, we compared modulation of KCNQ1 by tagged versus untagged KCNE1. For these tests, cRNA encoding either tagged or nontagged KCNE1 was microinjected into oocytes along with cRNA encoding KCNQ1, followed by electrophysiological examination of channel properties. It was observed that both untagged and His$_6$-tagged KCNE1 led to dramatically increased KCNQ1 conductance while also slowing the rate of current activation (Figure 2), which reflects the formation of a functional complex between KCNE1 and KCNQ1. Current−voltage relationships and normalized isochronal activation curves were observed to be very similar for tagged and nontagged KCNE1. Figure 2C illustrates normalized isochronal activation data fit with a Boltzmann distribution to obtain apparent $V_{1/2}$ and slope (k_V) factors. The calculated values for KCNQ1 and untagged KCNE1 are as follows: $V_{1/2} = 28.1 \pm 1.5$ and $k_V = 21.5 \pm 1.2$. Values for KCNQ1 and His$_6$-KCNE1 were not significantly different: $V_{1/2} = 27.0 \pm 1.6$ and $k_V = 23.6 \pm 1.2$. The presence of a His$_6$ tag does not affect the ability of KCNE1 to modulate KCNQ1.

Microinjection of KCNE1 in Detergent Micelle Solutions into Xenopus Oocytes. A concern regarding KCNE1 in detergent micelles is whether it is correctly folded or whether it might instead be irreversibly misfolded. Although KCNE1 has no known independent function, its integrity following purification and reconstitution can be determined by assessing its modulation of KCNQ1. We therefore injected purified His$_6$-KCNE1 into *Xenopus* oocytes expressing KCNQ1 channels. Figure 3 shows representative whole-cell currents recorded when KCNQ1-expressing oocytes were injected with recombinant KCNE1 in micelles (with dilution to well below the critical micelle concentration of the detergent). Injection of His$_6$-KCNE1 from DPC (Figure 3A) and SDS (Figure 3B) micelles did not alter the function of KCNQ1 channels (see Figure 2A). Whether this lack of function was the result of irreversible misfolding of KCNE1 in SDS and DPC or whether these detergents are simply unable to deliver and facilitate insertion of KCNE1 into oocyte membranes was not established by these results. In contrast, injection of His$_6$-KCNE1 from PMAL-C12 (Figure 3C), DTAB (Figure 3D), LMPC/LMPG (4:1, Figure 3E), or LMPG (Figure 3F) solutions into oocytes altered KCNQ1 activity in a manner similar to that of His$_6$-KCNE1 expressed from cRNA (Figure 2A): whole-cell current increased and current activation was delayed. While functional interaction of purified His$_6$-KCNE1 with KCNQ1 was also observed with LMPC/G, PMAL-C12, and DTAB, the greatest increase in current magnitude and the most reduced rate of current activation were observed when His$_6$-KCNE1 was injected from LMPG micelles (Figure 3F). For all the compounds that were tested, injection of micelles devoid of protein did not alter KCNQ1 channel activity (data not shown). It should be noted that the number of dead or leaky oocytes (see Materials and Methods) was much higher following injection of SDS or DPC micelles (with or without KCNE1) relative to LMPG, LMPC/G, PMAL-C12, and DTAB.

Viability of His$_6$-KCNE1 in LMPG Micelles. Figure 4 shows representative whole-cell currents recorded from oocytes injected with cRNA for KCNQ1 (A) or cRNA for both KCNQ1 and His$_6$-KCNE1 (B, "positive control"). Injection of "empty" LMPG micelles did not affect the properties of KCNQ1 channels (Figure 4C). In contrast, injection of purified His$_6$-KCNE1 in LMPG led to whole-cell currents (Figure 4D) that resembled the current recorded from oocytes injected with cRNA for both KCNQ1 and His$_6$-KCNE1 (Figure 4B). The increases in the current amplitude (Figure 4E) and voltage dependence of activation (Figure 4F) were similar, whether cRNA for His$_6$-KCNE1 or recombinant protein was injected. Collectively, these results demonstrated that recombinant His$_6$-KCNE1 in LMPG micelles was not irreversibly misfolded and that micelles of this type were able to effectively deliver KCNE1 to oocyte membranes, where it then inserted and modulated KCNQ1 function in a nativelike manner.

In contrast to the case for LMPG, the results for SDS and DPC fall short of validating the use these types of micelles as suitable media for structural studies of KCNE1. Results for the other systems that were tested (LMPC/LMPG, DTAB, and PMAL-C12) indicated no cause for concern, although LMPG was observed to be optimal.

2D NMR Spectra of KCNE1 in Different Micelles. Because KCNE1 is only weakly soluble in PMAL-C12 or DTAB,

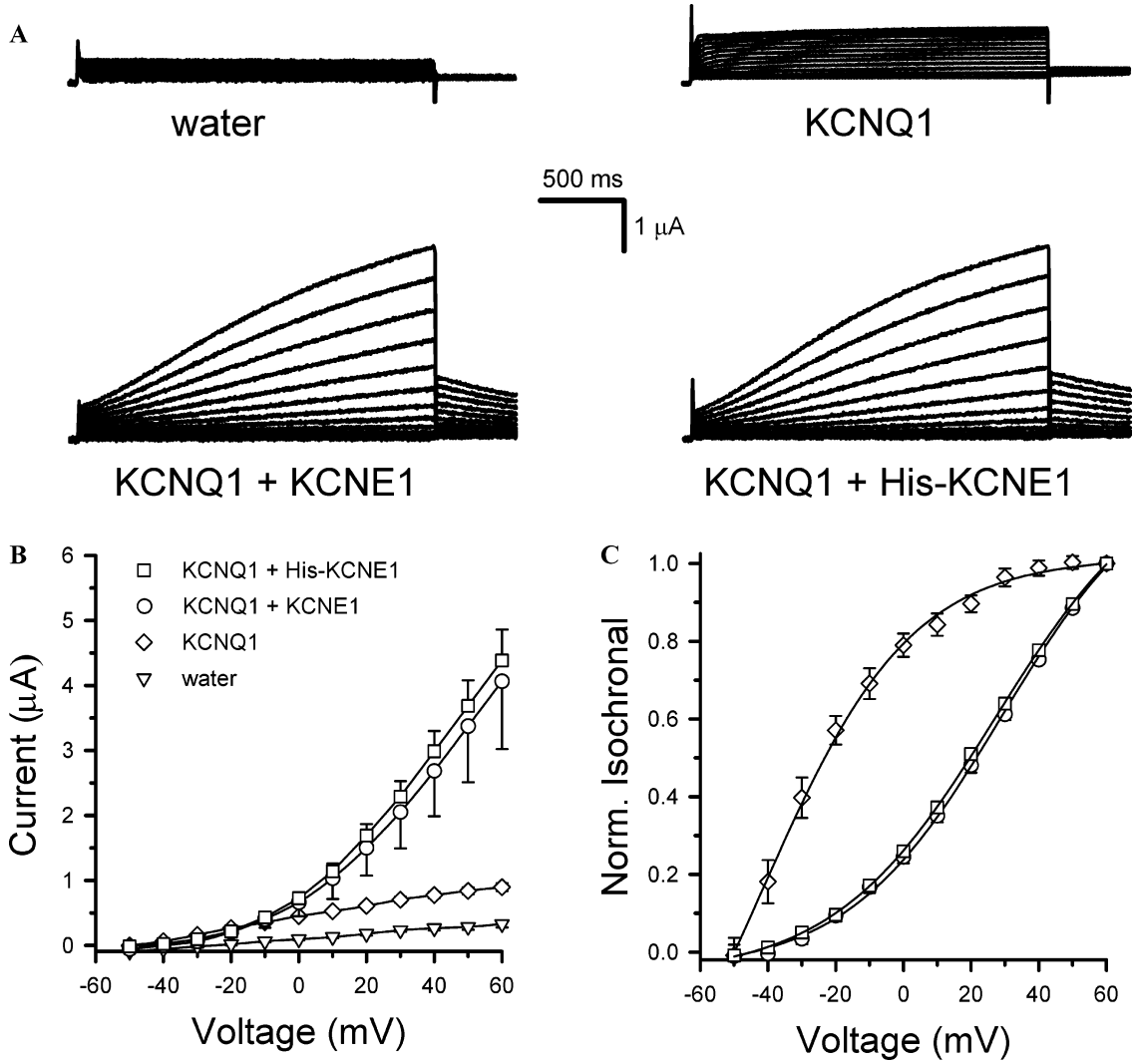

FIGURE 2: Functional expression of His_6-KCNE1 in *Xenopus* oocytes. (A) Representative current traces recorded from oocytes injected with either water ($N = 9$), cRNA for KCNQ1 only ($N = 12$), cRNA for both KCNQ1 and untagged KCNE1 ($N = 8$), or cRNA for both KCNQ1 and His_6-KCNE1 ($N = 10$). (B) Current−voltage relationship for currents measured after 2 s test pulses from a holding potential of −80 mV. (C) Normalized isochronal activation curves for oocytes injected with either water or cRNA. Data were fit with a Boltzmann function.

we did not attempt to acquire NMR spectra in these media but focused instead on LMPG and on a 4:1 LMPC/LMPG mixture. For the sake of comparison, spectra were also acquired in SDS and DPC. The 600 MHz TROSY NMR spectra of the four samples are shown in Figure 5. While all four spectra were of reasonably high quality on the basis of the number of peaks resolved, the spectra from LMPG and SDS are clearly superior, in each case yielding roughly one amide $^1H-^{15}N$ TROSY cross-peaks for each residue of KCNE1. The spectrum for the LMPG sample was superior to that of SDS in that peak line widths were much more uniform than for SDS. In the SDS case, there are a number of low-intensity (broad) peaks that can be observed only when the spectrum is plotted at a high vertical scale, as shown.

The combination of the fact that few peaks were observed at >8.9 or <7.3 ppm in any of the four spectra and spectral quality was reasonably high in all cases suggests that KCNE1 is a mostly helical protein under a broad range of micellar conditions.

NMR Assignments and Dynamics of KCNE1 in LMPG Micelles. Given the favorable oocyte injection results for KCNE1 and LMPG and the particularly high quality of the TROSY NMR spectrum of the protein from this mixture, we proceeded to use a suite of 3D TROSY-based heteronuclear NMR experiments to assign the backbone resonances of uniformly ^2H-, ^{13}C-, and ^{15}N-labeled His_6-KCNE1 in LMPG micelles. Ambiguities in assignment were clarified by labeling the protein with a series of specific ^{15}N-labeled amino acids (e.g., Cys, Met, Leu, Ile, Val, Trp, or Phe) and then recording TROSY spectra for each sample. Nearly complete H(N), N, CO, and C_α assignments (94%) as well as 84% of C_β assignments were obtained and have been deposited in the BioMagResBank as entry 15102. The assigned 900 MHz $^1H-^{15}N$ TROSY spectrum is shown in Figure 6. Preliminary TALOS analysis (*46*) of the chemical shifts led to determination of α-helices spanning sites 9−23, 46−58, 62−69, and 93−105. This analysis is preliminary in the sense that chemical shift analysis is more reliable when H_α chemical shifts are available, which they are not for KCNE1 (because backbone heteroatom assignments required the use of perdeuterated protein).

With assignments in hand, we proceeded to collect a set of ^{15}N T_1, T_2, and steady-state $^1H-^{15}N$ NOE measurements

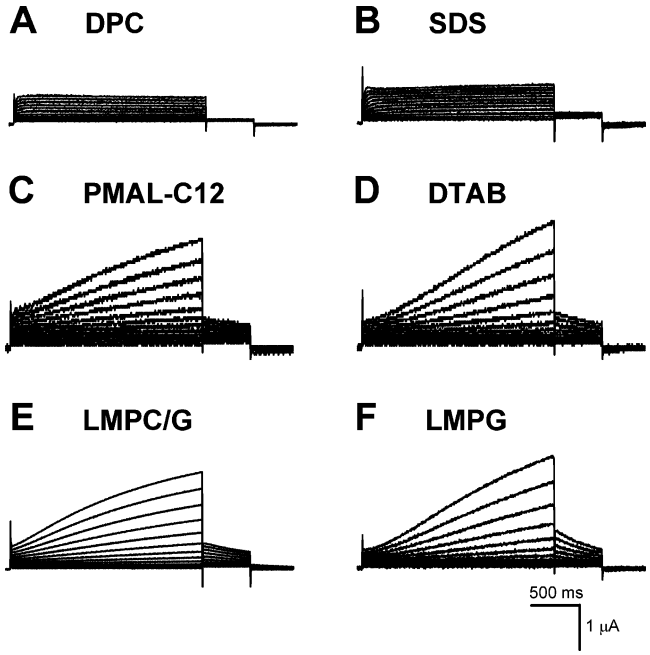

FIGURE 3: Representative current traces recorded from oocytes treated with cRNA for KCNQ1 and purified recombinant His_6-KCNE1 protein in different detergents: (A) DPC ($N = 8$), (B) SDS ($N = 9$), (C) PMAL-C12 ($N = 5$), (D) DTAB ($N = 6$), (E) LMPC/LMPG (4:1 molar ratio; $N = 7$), and (F) LMPG ($N = 9$).

at 600 MHz. These measurements are illustrated in Figure 7. The standard deviations associated with most points are considerable, reflecting both the modest signal-to-noise ratio observed in spectra of KCNE1 and difficulties in resolving peaks in the 2D relaxation data sets. To assess the reliability of the 600 MHz measurements, we repeated relaxation experiments at 800 MHz (Figure 2 of the Supporting Information). While the 800 MHz measurements also exhibit considerable experimental uncertainties, there is generally good agreement with the 600 MHz measurements of Figure 7.

From the T_1/T_2 ratio plateau for the transmembrane domain (residues 44−66), it is possible to calculate an overall correlation time for the KCNE1−LMPG complex of roughly 21 ns, which is consistent with a protein−micelle aggregate molecular mass in the range of 60 kDa. The positive NOE values for residues 1−105 suggest that the N-terminus, transmembrane domain, and juxtamembrane C-terminus (residues 67−105) contain considerable ordered structure, although both NOE and T_1/T_2 indicate significant local flexibility at a number of segments within this span, most obviously at sites spanning sites 1−10 and 23−43, but also including sites 58, 59, and 61 in the transmembrane domain. Site 62 also exhibits unusual dynamics in that its amide $^1H-^{15}N$ peak is undetectably broad, most likely due to intermediate time scale conformational exchange. The degree of order in the C-terminus of KCNE1 is seen to fall off starting after residue 105, with mobility increasing as the extreme C-terminus is approached. This region of the protein appears to be largely disordered.

DISCUSSION

Microinjection of Recombinant KCNE1 into Xenopus Oocytes. Previous studies have demonstrated the successful incorporation of membrane proteins into oocyte membranes following microinjection of solutions containing protein in membrane vesicles (*47*−*49*). In those studies, the vesicles evidently either spontaneously fused with oocyte membranes or were actively engaged by the membrane fusion machinery of the cell. Here, is has been shown that is possible for a membrane protein to be successfully integrated into oocyte membranes following microinjection of the protein as a micellar solution. The exact routes taken by the injected KCNE1 for insertion into the host oocyte membranes, the location of the organelle at which it co-assembles with the channel, and the membrane trafficking routes potentially taken by KCNE1 or KCNE1 and KCNQ1 to reach the plasma membrane are being investigated. On the basis of the fact that some membrane proteins have the capacity to spontaneously insert into intact lipid vesicles when diluted from micelles, amphipols, or denaturant solutions (cf., refs *50*−*52*), it is possible that insertion of KCNE1 into oocyte membranes may not require engagement with the cellular membrane protein insertion machinery.

In addition to using detergents to deliver KCNE1 to oocyte membranes, we also found that the zwitterionic amphipol PMAL-C12 was also an effective KCNE1 carrier. This represents the second report that amphipols can deliver an otherwise "naked" membrane protein into preformed lipid bilayers (*51*). Unlike detergents, amphipols will remain complexed with membrane proteins in aqueous solution even at very low concentrations and may therefore be especially appropriate membrane protein carrier agents for conditions under which a purified membrane protein needs to be diluted manyfold into detergent-free solution (*53*, *54*). Amphipols have also been shown to be capable of sustaining the native functionality of membrane proteins (*53*, *55*, *56*).

Recombinant KCNE1 was seen to attain its fully functional state in oocytes when it was injected from LMPG or, to a lesser degree, LMPC and LMPG (4:1), DTAB, or amphipol PMAL-C12 solutions, but not from DPC or SDS. There are two most-likely explanations for the latter observation. First, it is possible that KCNE1 was either terminally misfolded in DPC or SDS or so destabilized in these micelle types that when it did bind to the native membranes it was in an "off-pathway" folding potential state, leading to misfolding. We cannot completely rule this out, but our NMR results (Figure 5) disfavor this interpretation. The TROSY spectra of KCNE1 in SDS and DPC suggest that KCNE1 in these micelles is effectively structurally homogeneous; if there are multiple conformations, they must be in rapid exchange with each other, not kinetically trapped in misfolded states (leading to extra sets of peaks or peak disappearances). Moreover, the NMR spectra from SDS and DPC bear some general similarity to the spectrum of KCNE1 in LMPG, for which more favorable functional results were obtained after microinjection. This suggests that the structure of KCNE1 in SDS or DPC bears some resemblance to that in LMPG.

An alternative explanation for why KCNE1 does not reach its functional state after microinjection from SDS or DPC solutions is that these detergents are unable to facilitate delivery and/or insertion of KCNE1 into oocyte membranes. One possibility is that when KCNE1 in DPC or SDS micelles is microinjected into oocytes the detergent rapidly dissociates to monomer from KCNE1 as a consequence of dilution below the CMC, leading to aggregation before the protein has a chance to reach the membrane in which it might

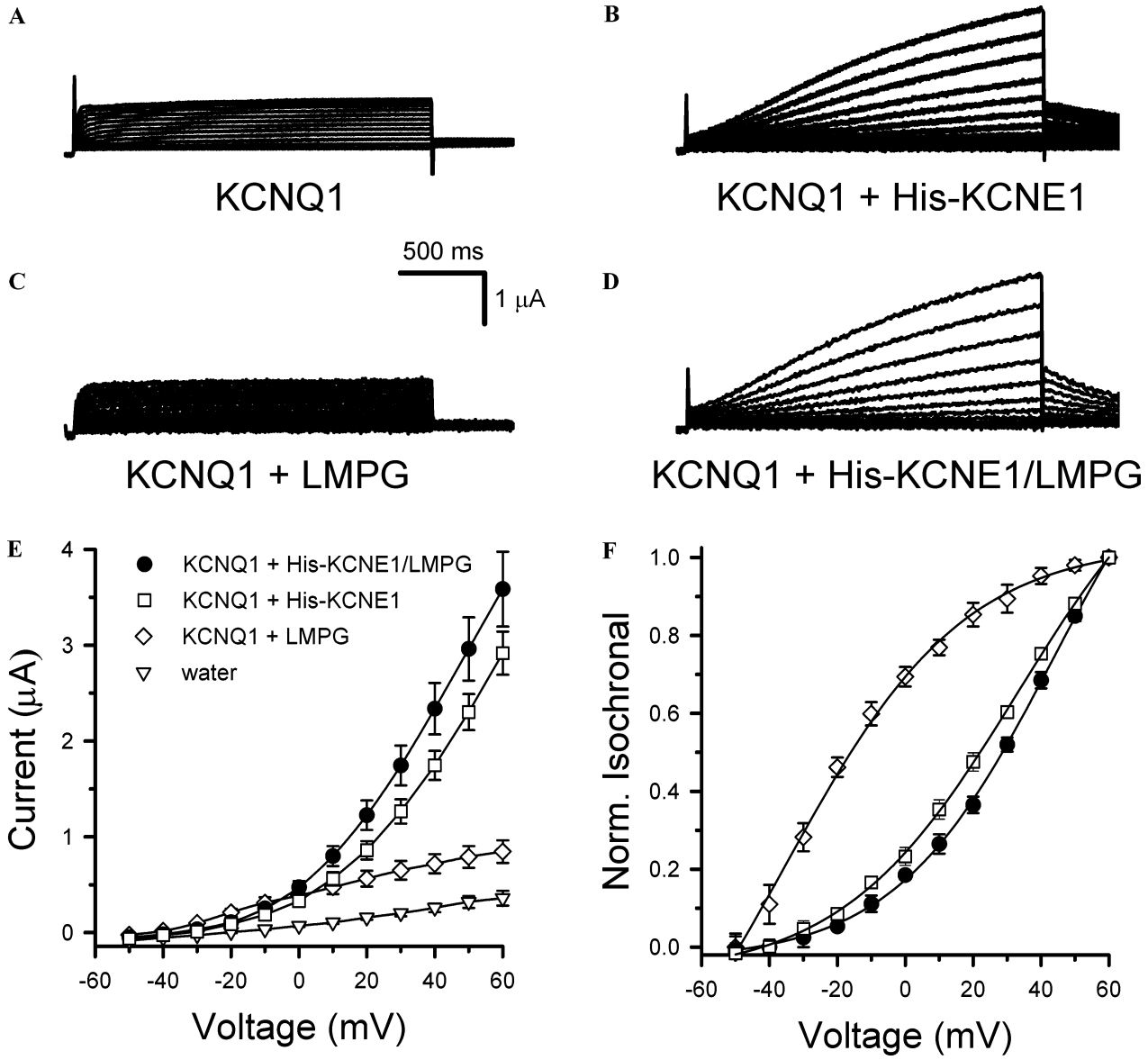

FIGURE 4: Modulation of KCNQ1 channels in *Xenopus* oocytes. Representative current traces recorded from oocytes injected with (A) cRNA for KCNQ1 only ($N = 6$), (B) cRNA for both KCNQ1 and His_6-KCNE1 ($N = 11$), (C) cRNA for KCNQ1 and LMPG micelles (no KCNE1; $N = 17$), and (D) cRNA for KCNQ1 with purified His_6-KCNE1 in LMPG micelles ($N = 10$). Oocytes were injected with cRNAs or water, followed 24 h later by injection with either "empty" or His_6-KCNE1-containing 0.1% LMPG micelles. Currents were then recorded 24 h after the second injection. (E) Current−voltage relationship measured after 2 s pulses from oocytes that were injected with either water ($N = 13$), cRNA for KCNQ1 and LMPG micelles (no KCNE1), cRNA for both KCNQ1 and His_6-KCNE1, or cRNA for KCNQ1 and purified His_6-KCNE1 in LMPG micelles. (F) Normalized isochronal activation curves for oocytes injected with cRNA for KCNQ1 and LMPG micelles (no KCNE1), cRNA for both KCNQ1 and His_6-KCNE1, or cRNA for KCNQ1 and purified His_6-KCNE1 in LMPG micelles. A fit of these data to Boltzman distributions resulted in the following fit parameters: cRNA KCNQ1 and LMPG micelles (no KCNE1), $V_{1/2} = -34.3 \pm 3.2$ and $k_V = 20.9 \pm 2.2$; cRNA for both KCNQ1 and His_6-KCNE1, $V_{1/2} = 28.5 \pm 0.7$ and $k_V = 20.6 \pm 0.6$; and cRNA for KCNQ1 and purified His_6-KCNE1 in LMPG micelles, $V_{1/2} = 32.1 \pm 1.7$ and $k_V = 23.5 \pm 1.1$.

otherwise insert. This explanation is unlikely. The CMCs for SDS (7 mM) and DPC (2 mM) are actually slightly lower than that of DTAB (8 mM) (*57*), the latter of which was found to efficiently deliver KCNE1 to oocyte membranes. A more likely explanation for the failure of SDS and DPC to deliver is that LMPG, LMPC and LMPG, DTAB, and PMAL-C12 play active roles in facilitating correct membrane insertion of KCNE1, whereas SDS and DPC do not. Elucidation of the exact nature of the insertion mechanisms will require further study.

The ability to inject recombinant KCNE1 into oocytes from micellar solutions would appear to open the door to a host of applications, such as those that would exploit chemical tagging of KCNE1 prior to microinjection, experiments that are not feasible using standard molecular biology expression methods. However, choice of a suitable micellar solution is critical. Not all micellar solutions are tolerated well by oocytes. Among the six detergents and amphipols examined herein, injection of SDS or DPC micelles caused a large number of oocytes to become irreversibly leaky (see the Results). Recombinant KCNE1 in LMPC/G, PMAL-C12, and DTAB was observed to be able to co-assemble with the KCNQ1 channel. However, for these systems, the degree of channel modulation by KCNE1 was lower than when LMPG was used, suggesting higher efficiency of co-assembly in the latter case.

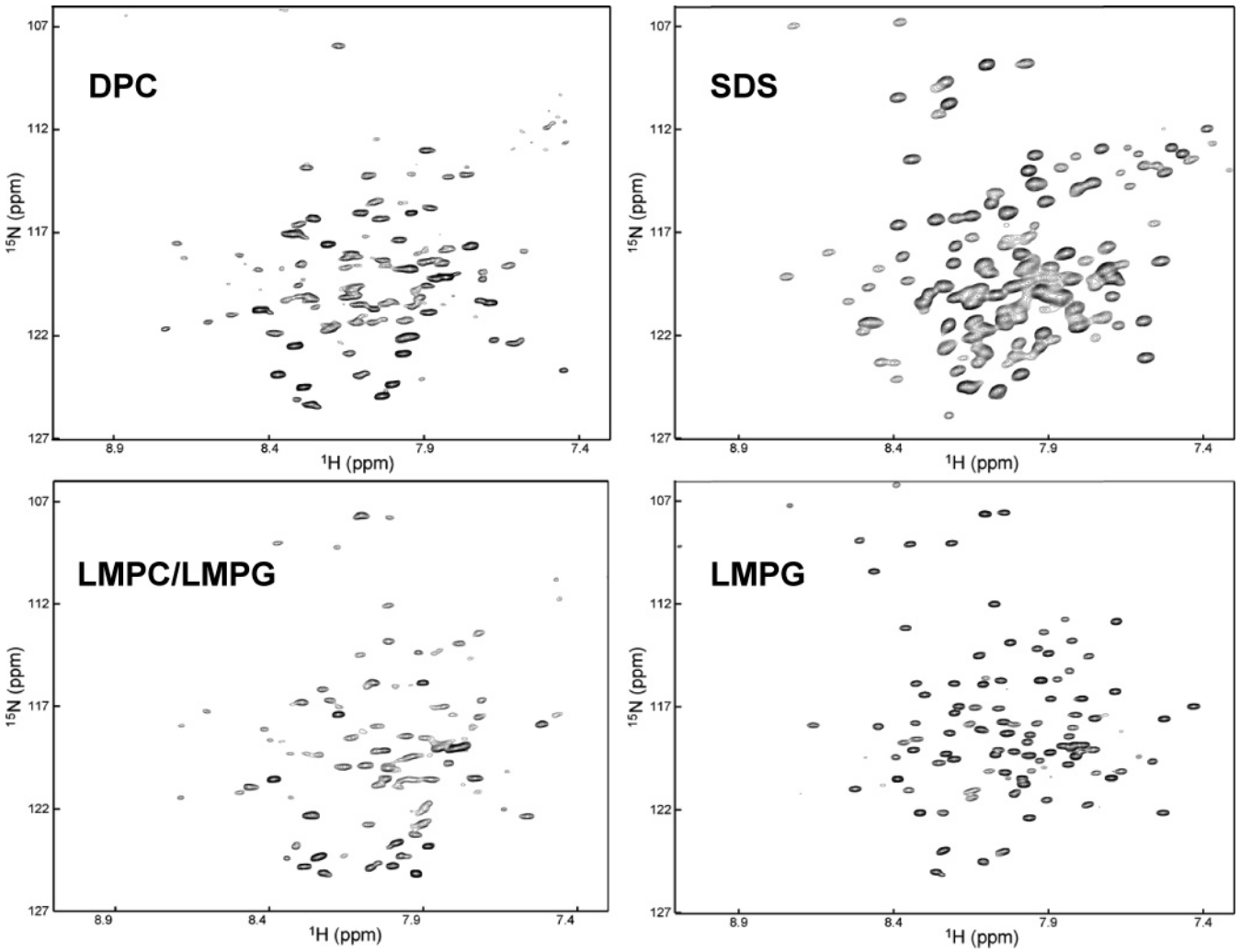

FIGURE 5: 2D 600 MHz ^{1}H−^{15}N TROSY NMR spectra of purified [U-^{15}N]His$_6$-KCNE1 at 1−1.5 mM in different detergent micelles. Samples contained 250 mM imidazole, 2 mM DTT, and 2 mM EDTA (pH 6.0). All the spectra were acquired with 256 × 1024 complex points (prior to zero-filling) at 40 °C. Data were processed using zero-filling and Gaussian apodization in both dimensions (the same parameters were used in processing all four spectra). The concentrations of detergents were as follows: (A) 300 mM DPC, (B) 300 mM SDS, (C) 150 mM LMPC/LMPG mixture (4:1 molar ratio), and (D) 150 mM LMPG. It should be noted that the line widths for most peaks in the SDS case are similar to those of LMPG. However, the SDS spectrum has been plotted at a higher scale than the LMPG spectrum (leading to the mistaken impression of broader peaks) to allow observation of a few weak peaks that would not be observed if the SDS spectrum was plotted at the same scale as the LMPG spectrum. An additional spectrum (not shown) acquired for KCNE1 in 300 mM DPC/SDS (10:1) closely resembled that of DPC alone (A). Overlays of the spectra for SDS, DPC, and the LMPC/LMPG mixture with the assigned spectrum for LMPG are provided as Supporting Information (Figure 1).

In general, the results from the KCNE1 injection studies provide a modest degree of validation for the biological integrity of conducting structural studies of this protein in LMPG micelles, in micellar LMPC/LMPG mixtures, in DTAB micelles, or in amphipol PMAL-C12. On the other hand, for SDS and DPC, the results can be regarded, at best, as being neutral on this question. Since KCNE1's solubility in DTAB and PMAL-C12 is only moderate, while being much higher in LMPG or in an LMPC/LMPG mixture, the oocyte injection results lead to a modest preference for lysophospholipid micelles as the medium for structural studies of KCNE1. Lysophospholipids are increasingly being used as a medium for structural biological investigations of membrane proteins (*58*−*62*). Among all detergents, the lysophospholipids are the most phospholipid-like (except, perhaps, for the short chain diglyceride phospholipids). It is therefore not surprising that the lysophospholipids, including LMPG, have been found to be exceptionally mild detergents in this work and in previous studies (*60*, *63*−*66*). This is in contrast to SDS, which denatures many proteins, including some (but not all) membrane proteins, whereas DPC is believed to be intermediate in harsh-to-mild detergent scale (see the review in ref *38*).

Preliminary NMR Studies Provide Insight into KCNE1 Structure and Dynamics. The fact that the spectra of the protein in LMPG and SDS are superior to spectra from DPC and the 4:1 LMPC/LMPG mixture suggests that there are intermediate time scale motions in these latter systems that result in severe line broadening for some resonances. However, all four spectra exhibit some general similarity (see Figure 5 and Figure 1 of the Supporting Information), suggesting a degree of structural commonality for KCNE1 in these systems. LMPG was chosen as the medium for ongoing structural studies of KCNE1 because it provides an excellent NMR spectrum and because it performed admirably in the oocyte injection studies (above). LMPG has also previously been shown to be an extremely effective detergent in maintaining nativelike structure and function in a complex

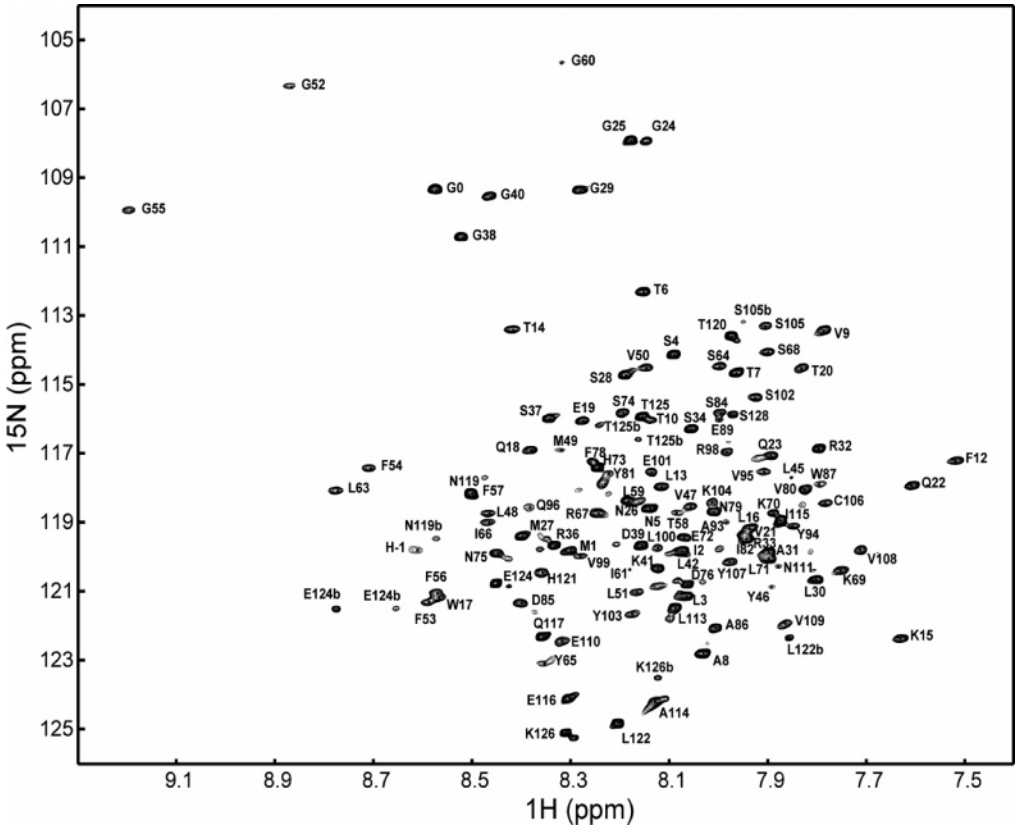

FIGURE 6: $^{1}H-^{15}N$ TROSY spectrum of uniformly ^{2}H-, ^{13}C-, and ^{15}N-labeled KCNE1 in 4% LMPG, 10% D_2O, 250 mM imidazole/acetic acid, 2 mM DTT, and 2 mM EDTA (pH 6.0). The spectrum was recorded at 40 °C on a 900 MHz spectrometer with 256 complex points in t_1, 1024 complex points in t_2, and four scans per increment. Backbone amide resonance assignments are indicated by the one-letter amino acid code and the sequence number. The cross-peaks for 119b, 122b, 124b, 125b, and 126b represent the presence of a second conformation that is spectroscopically detectable for those residues as a result of cis−trans isomerization for the neighboring Pro residues (Pro118, Pro123, and Pro127) in the flexible distal C-terminus. The cross-peaks for His(−1) and Gly0 represent the residues linking the N-terminal purification tag to the first residue (Met1) of KCNE1 proper. The assignment for site 93 remains tentative.

membrane protein (*66*) and has also been shown to be useful as a medium for NMR studies of other membrane proteins (*58*, *60*, *67*). That LMPG was observed to be nearly as effective as SDS at solubilizing KCNE1 (see Materials and Methods) is most likely due to the fact that it also has an anionic headgroup. However, LMPG is milder than SDS in terms of disrupting native protein structure, probably because it has a polar but uncharged spacer, glycerol, separating its apolar tail and charged headgroup.

The relatively narrow $^{1}H-^{15}N$ peak chemical shift dispersion observed for KCNE1 in LMPG micelles is characteristic of largely α-helical proteins. This modest chemical shift dispersion combined with the significant size of the KCNE1−LMPG micellar complex dictated that completion of assignments required use of very high magnetic fields, TROSY-based NMR pulse sequences (*68*), and supplementation of 3D spectra with 2D TROSY data from ^{15}N amino acid specifically labeled protein. Backbone NMR resonance assignments for KCNE1 in LMPG micelles were completed. TALOS-based analysis of the backbone chemical shifts confirms that at least 50 residues are part of α-helices. The resonance assignments provide a basis for ongoing efforts to determine the three-dimensional structure of KCNE1.

NMR relaxation measurements indicated that KCNE1's distal C-terminus (residues 106−129) is much more flexible than the rest of the protein and is largely disordered. This is not surprising since it has been shown that residues 94 and higher can be deleted from KCNE1 without disrupting its ability to modulate KCNQ1 K_V channel function (*29*). It is, however, interesting to point out that this domain includes two known sites for mutations that result in long QT syndrome (Val109 and Pro127). We speculate that while the distal C-terminus is disordered under the conditions of our NMR studies and does not interact directly with KCNQ1, this very disorder makes this segment particularly accessible for participation in protein−protein interactions under cellular conditions. It was recently discovered that the cytosolic domain of KCNE1 interacts with a sarcomeric adaptor protein, T-cap (also know as telethonin), in a manner that may link KCNE1's modulation of KCNQ1 channel function to the protein assemblies involved in cardiac muscle contraction (*69*). While our results do not prove that the distal C-terminus of KCNE1 is crucial to interaction with T-cap, this domain would appear to be well-suited to being a candidate for participation in such interactions.

In addition to revealing a mobile distal C-terminus, the NMR relaxation measurements suggest that residues 9−23, which comprise an α-helix, are nearly as immobile as most of the transmembrane domain (residues 44−66), which might reflect association of this segment with the micelle surface. This possibility is supported by a helical wheel plot (not shown), which indicates this segment is an amphipathic helix.

The α-Helicity of the Transmembrane Segment of KCNE1 in LMPG Micelles Is Interrupted Near Functionally Critical Residues 57−59. Previous studies of a polypeptide corresponding to the transmembrane segment of KCNE1 indicated

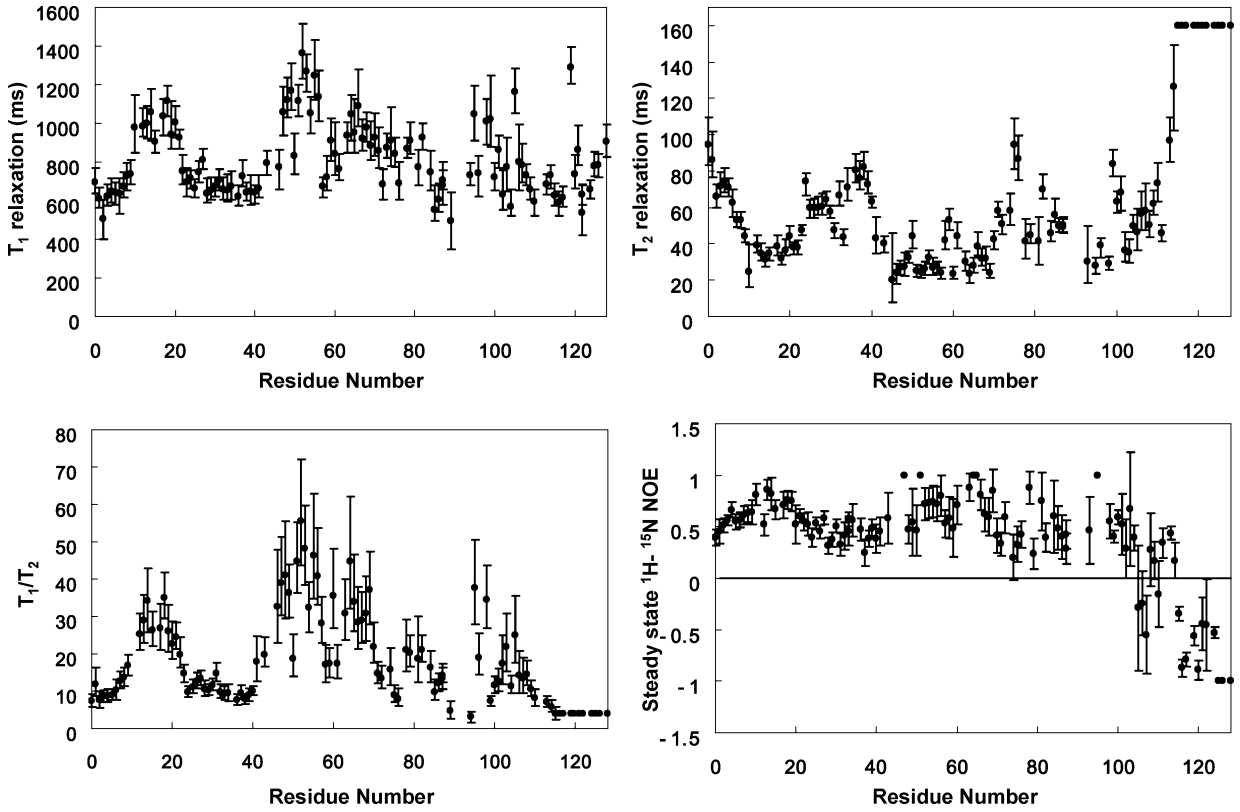

FIGURE 7: NMR relaxation parameters (600 MHz) for His_6-KCNE1 in LMPG micelles at 40 °C. Values reported with no error bars represent measurements for which only lower boundary (T_2) or upper boundary (T_1/T_2 and |NOE|) values could be determined. Sites for which no values are reported represent residues for which assignments were not available or for which extensive resonance overlap hindered the extraction of reliable parameters. The corresponding data at 800 MHz are provided as Supporting Information (Figure 2).

that this polypeptide was largely α-helical in a variety of different model membrane systems, unless conditions were such that the peptide aggregated, in which case aberrant *β*-sheet structure was observed (*31*−*35*). These previous studies included a careful NMR study that showed the isolated TM segment of KCNE1 in an 86:14 hexafluoro-2-propanol/water mixture forms a single unbroken α-helix (*32*). The results of this work are in general agreement with these previous observations in that we also observed that the majority of the KCNE1 transmembrane segment is helical. However, in contrast to the conclusions of the previous NMR study, our results for intact KCNE1 in LMPG micelles show that its TM helix is interrupted by a nonhelical mobile segment located roughly between sites 59 and 61. The variance of the results from these two studies most likely reflects the different model membrane media in which they were carried out. This begs the question of which system, LMPG micelles or a hexafluoro-2-propanol/water mixture, is closest to nativelike conditions for KCNE1.

While we have argued that LMPG micelles represent an especially suitable membrane-mimetic medium, it should be considered that even lipid bilayers would not represent a truly nativelike environment for KCNE1 in its functionally relevant form. It is believed that KCNE1 associates with the KCNQ1 channel early in the secretory pathway and most likely remains stably associated with the channel (*70*, *71*). In this state, it is probable that one face of the KCNE1 transmembrane segment is lipid-exposed but that the other face interacts with KCNQ1, conditions that are impossible to ideally mimic for isolated KCNE1 in any model membrane system. We hypothesize that KCNE1's transmembrane segment has a propensity for being completely helical but that that sites 59−61 have a helical propensity much lower than that of the rest of the segment. As a consequence, under some conditions (such as in LMPG micelles), it adopts a nonhelical conformation. While a break in a TM helix might normally be regarded as energetically abhorrent because of the loss of backbone amide hydrogen bonding in a highly apolar environment, this is a smaller problem in detergent micelles, which are much more water-saturated than lipid bilayers. Local loss of helicity for KCNE1 in its native complex with KCNQ1 would also be energetically feasible under native conditions if loss of classical helical backbone hydrogen bonds were offset by a rearrangement of hydrogen bonding partners within KCNE1 or through formation of favorable KCNQ1−KCNE1 interactions that satisfied KCNE1's hydrogen bonding potential around sites 59−61.

It is not structurally obvious why residues 59−61 exhibit the unusual property of having only moderate helical propensity in a hydrophobic environment. The presence of a number of *β*-branched amino acids combined with two Gly residues in or near this segment may be a contributing factor. Another contributing factor in the highly dynamic and internally permeable environment of micelles is that the side chain hydroxyl of Thr58 might transiently hydrogen bond with either water, backbone amide groups within the adjacent nonhelical segments, or oxygen present in the glycerol/headgroup regions of LMPG.

Because the nonhelical residues 59−61 of KCNE1 overlaps with sites 57−59, which are believed to be critical to modulation of KCNQ1 channel function, it is possible that the distinctive conformational and dynamic properties of this

segment may be of the highest functional relevance. Sites 57−59 of KCNE1 are essential in defining how KCNE1 regulates channel function in a manner that is distinct from those of other KCNE family members (*13*, *25*−*27*). It is believed that this segment interacts directly with the S6 segment of the pore domain, with Thr58 being especially important. Swapping these three sites out of KCNE1 for the corresponding sites in KCNE3 converts the triple mutant KCNE1 into a KCNE3-like modulator of KCNQ1 function (*25*). Namely, while channel conductance is dramatically increased by the presence of this triple mutant form of KCNE1 (just as for the wild type), the delay in voltage-stimulated channel activation that is normally imposed by wild-type KCNE1 is completely absent. This matches what is observed when bona fide KCNE3 serves as the β-subunit (*21*). Further elucidation of how the local dynamics near site 59 are related to modulation of KCNQ1 by KCNE1 will await completion of KCNE1's complete structure. However, the results of this work suggest that this segment may be able to interact with the transmembrane domain of the channel via an alternative mode to classical helix−helix interactions. The fact that this segment of KCNE1 also can access both helical and nonhelical conformations, depending on the details of its nonpolar medium, also suggests the feasibility that as the KCNQ1 channel undergoes transitions between open and closed conformational states, the TM domain of KCNE1 could also undergo changes in conformation that are centered in the vicinity of residue 59.

ACKNOWLEDGMENT

We thank Dr. Fang Tian of the University of Georgia (Athens, GA) for collecting the 900 MHz NMR data, Arina Hadziselimovic for help with molecular biology, Prof. Frank Sönnichsen for helpful discussion, and Markus Voehler and Dr. Murthy Karra for NMR technical assistance.

SUPPORTING INFORMATION AVAILABLE

Superimposed TROSY spectra of KCNE1 in LMPG with other detergents (Figure 1) and 800 MHz relaxation measurements for KCNE1 in LMPG micelles (Figure 2). This material is available free of charge via the Internet at http://pubs.acs.org.

REFERENCES

1. Jespersen, T., Grunnet, M., and Olesen, S. P. (2005) The KCNQ1 potassium channel: From gene to physiological function, *Physiology (Bethesda) 20*, 408−416.
2. Robbins, J. (2001) KCNQ potassium channels: Physiology, pathophysiology, and pharmacology, *Pharmacol. Ther. 90*, 1−19.
3. Martens, J. R., Kwak, Y. G., and Tamkun, M. M. (1999) Modulation of Kv channel α/β subunit interactions, *Trends Cardiovasc. Med. 9*, 253−258.
4. Pongs, O., Leicher, T., Berger, M., Roeper, J., Bahring, R., Wray, D., Giese, K. P., Silva, A. J., and Storm, J. F. (1999) Functional and molecular aspects of voltage-gated K^+ channel β subunits, *Ann. N.Y. Acad. Sci. 868*, 344−355.
5. Rettig, J., Heinemann, S. H., Wunder, F., Lorra, C., Parcej, D. N., Dolly, J. O., and Pongs, O. (1994) Inactivation properties of voltage-gated K^+ channels altered by presence of β-subunit, *Nature 369*, 289−294.
6. Trimmer, J. S. (1998) Regulation of ion channel expression by cytoplasmic subunits, *Curr. Opin. Neurobiol. 8*, 370−374.
7. An, W. F., Bowlby, M. R., Betty, M., Cao, J., Ling, H. P., Mendoza, G., Hinson, J. W., Mattsson, K. I., Strassle, B. W., Trimmer, J. S., and Rhodes, K. J. (2000) Modulation of A-type potassium channels by a family of calcium sensors, *Nature 403*, 553−556.
8. Pourrier, M., Schram, G., and Nattel, S. (2003) Properties, expression and potential roles of cardiac K^+ channel accessory subunits: MinK, MiRPs, KChIP, and KChAP, *J. Membr. Biol. 194*, 141−152.
9. McCrossan, Z. A., and Abbott, G. W. (2004) The MinK-related peptides, *Neuropharmacology 47*, 787−821.
10. Abbott, G. W., Sesti, F., Splawski, I., Buck, M. E., Lehmann, M. H., Timothy, K. W., Keating, M. T., and Goldstein, S. A. (1999) MiRP1 forms IKr potassium channels with HERG and is associated with cardiac arrhythmia, *Cell 97*, 175−187.
11. Abbott, G. W., Goldstein, S. A. N., and Sesti, F. (2001) Do all voltage-gated potassium channels use MiRPs? *Circ. Res. 88*, 981−983.
12. Barhanin, J., Lesage, F., Guillemare, E., Fink, M., Lazdunski, M., and Romey, G. (1996) K(V)LQT1 and lsK (minK) proteins associate to form the I(Ks) cardiac potassium current, *Nature 384*, 78−80.
13. Melman, Y. F., Krumerman, A., and McDonald, T. V. (2002) A single transmembrane site in the KCNE-encoded proteins controls the specificity of KvLQT1 channel gating, *J. Biol. Chem. 277*, 25187−25194.
14. Sanguinetti, M. C., Curran, M. E., Zou, A., Shen, J., Spector, P. S., Atkinson, D. L., and Keating, M. T. (1996) Coassembly of K(V)LQT1 and minK (IsK) proteins to form cardiac I(Ks) potassium channel, *Nature 384*, 80−83.
15. Napolitano, C., Priori, S. G., Schwartz, P. J., Bloise, R., Ronchetti, E., Nastoli, J., Bottelli, G., Cerrone, M., and Leonardi, S. (2005) Genetic testing in the long QT syndrome: Development and validation of an efficient approach to genotyping in clinical practice, *JAMA, J. Am. Med. Assoc. 294*, 2975−2980.
16. Abbott, G. W., and Goldstein, S. A. (2002) Disease-associated mutations in KCNE potassium channel subunits (MiRPs) reveal promiscuous disruption of multiple currents and conservation of mechanism, *FASEB J. 16*, 390−400.
17. Splawski, I., Tristani-Firouzi, M., Lehmann, M. H., Sanguinetti, M. C., and Keating, M. T. (1997) Mutations in the hminK gene cause long QT syndrome and suppress IKs function, *Nat. Genet. 17*, 338−340.
18. Wang, Q., Curran, M. E., Splawski, I., Burn, T. C., Millholland, J. M., VanRaay, T. J., Shen, J., Timothy, K. W., Vincent, G. M., de Jager, T., Schwartz, P. J., Toubin, J. A., Moss, A. J., Atkinson, D. L., Landes, G. M., Connors, T. D., and Keating, M. T. (1996) Positional cloning of a novel potassium channel gene: KVLQT1 mutations cause cardiac arrhythmias, *Nat. Genet. 12*, 17−23.
19. Abbott, G. W., and Goldstein, S. A. (2001) Potassium channel subunits encoded by the KCNE gene family: Physiology and pathophysiology of the MinK-related peptides (MiRPs), *Mol. Interventions 1*, 95−107.
20. Tinel, N., Diochot, S., Lauritzen, I., Barhanin, J., Lazdunski, M., and Borsotto, M. (2000) M-type KCNQ2-KCNQ3 potassium channels are modulated by the KCNE2 subunit, *FEBS Lett. 480*, 137−141.
21. Schroeder, B. C., Waldegger, S., Fehr, S., Bleich, M., Warth, R., Greger, R., and Jentsch, T. J. (2000) A constitutively open potassium channel formed by KCNQ1 and KCNE3, *Nature 403*, 196−199.
22. McCrossan, Z. A., Lewis, A., Panaghie, G., Jordan, P. N., Christini, D. J., Lerner, D. J., and Abbott, G. W. (2003) MinK-related peptide 2 modulates Kv2.1 and Kv3.1 potassium channels in mammalian brain, *J. Neurosci. 23*, 8077−8091.
23. McDonald, T. V., Yu, Z., Ming, Z., Palma, E., Meyers, M. B., Wang, K. W., Goldstein, S. A., and Fishman, G. I. (1997) A minK-HERG complex regulates the cardiac potassium current I(Kr), *Nature 388*, 289−292.
24. Chen, H., Kim, L. A., Rajan, S., Xu, S., and Goldstein, S. A. (2003) Charybdotoxin binding in the I(Ks) pore demonstrates two MinK subunits in each channel complex, *Neuron 40*, 15−23.
25. Melman, Y. F., Domenech, A., de la, L. S., and McDonald, T. V. (2001) Structural determinants of KvLQT1 control by the KCNE family of proteins, *J. Biol. Chem. 276*, 6439−6444.
26. Melman, Y. F., Um, S. Y., Krumerman, A., Kagan, A., and McDonald, T. V. (2004) KCNE1 binds to the KCNQ1 pore to regulate potassium channel activity, *Neuron 42*, 927−937.

27. Panaghie, G., Tai, K. K., and Abbott, G. W. (2006) Interaction of KCNE subunits with the KCNQ1 K^+ channel pore, *J. Physiol. 570*, 455−467.
28. Romey, G., Attali, B., Chouabe, C., Abitbol, I., Guillemare, E., Barhanin, J., and Lazdunski, M. (1997) Molecular mechanism and functional significance of the MinK control of the KvLQT1 channel activity, *J. Biol. Chem. 272*, 16713−16716.
29. Tapper, A. R., and George, A. L., Jr. (2000) MinK subdomains that mediate modulation of and association with KvLQT1, *J. Gen. Physiol. 116*, 379−390.
30. Tapper, A. R., and George, A. L., Jr. (2001) Location and orientation of minK within the I(Ks) potassium channel complex, *J. Biol. Chem. 276*, 38249−38254.
31. Aggeli, A., Boden, N., Cheng, Y. L., Findlay, J. B., Knowles, P. F., Kovatchev, P., and Turnbull, P. J. (1996) Peptides modeled on the transmembrane region of the slow voltage-gated IsK potassium channel: Structural characterization of peptide assemblies in the β-strand conformation, *Biochemistry 35*, 16213−16221.
32. Aggeli, A., Bannister, M. L., Bell, M., Boden, N., Findlay, J. B., Hunter, M., Knowles, P. F., and Yang, J. C. (1998) Conformation and ion-channeling activity of a 27-residue peptide modeled on the single-transmembrane segment of the IsK (minK) protein, *Biochemistry 37*, 8121−8131.
33. Ben Efraim, I., Bach, D., and Shai, Y. (1993) Spectroscopic and functional characterization of the putative transmembrane segment of the minK potassium channel, *Biochemistry 32*, 2371−2377.
34. Horvath, L. I., Knowles, P. F., Kovachev, P., Findlay, J. B., and Marsh, D. (1997) A single-residue deletion alters the lipid selectivity of a K^+ channel-associated peptide in the β-conformation: Spin label electron spin resonance studies, *Biophys. J. 73*, 2588−2594.
35. Mercer, E. A., Abbott, G. W., Brazier, S. P., Ramesh, B., Haris, P. I., and Srai, S. K. (1997) Synthetic putative transmembrane region of minimal potassium channel protein (minK) adopts an α-helical conformation in phospholipid membranes, *Biochem. J. 325* (Part 2), 475−479.
36. Korepanova, A., Gao, F. P., Hua, Y., Qin, H., Nakamoto, R. K., and Cross, T. A. (2005) Cloning and expression of multiple integral membrane proteins from *Mycobacterium tuberculosis* in *Escherichia coli*, *Protein Sci. 14*, 148−158.
37. Anantharam, A., Lewis, A., Panaghie, G., Gordon, E., McCrossan, Z. A., Lerner, D. J., and Abbott, G. W. (2003) RNA interference reveals that endogenous *Xenopus* MinK-related peptides govern mammalian K^+ channel function in oocyte expression studies, *J. Biol. Chem. 278*, 11739−11745.
38. Sanders, C. R., and Sonnichsen, F. (2006) Solution NMR of membrane proteins: Practice and challenges, *Magn. Reson. Chem. 44* (Special Issue), S24−S40.
39. Weigelt, J. (1998) Single scan, sensitivity- and gradient-enhanced TROSY for multidimensional NMR experiments, *J. Am. Chem. Soc. 120*, 10778−10779.
40. Delaglio, F., Grzesiek, S., Vuister, G. W., Zhu, G., Pfeifer, J., and Bax, A. (1995) NMRPipe: A multidimensional spectral processing system based on UNIX pipes, *J. Biomol. NMR 6*, 277−293.
41. Salzmann, M., Pervushin, K., Wider, G., Senn, H., and Wuthrich, K. (1998) TROSY in triple-resonance experiments: New perspectives for sequential NMR assignment of large proteins, *Proc. Natl. Acad. Sci. U.S.A. 95*, 13585−13590.
42. Johnson, B. A. (2004) Using NMRView to visualize and analyze the NMR spectra of macromolecules, *Methods Mol. Biol. 278*, 313−352.
43. Tugarinov, V., Hwang, P. M., and Kay, L. E. (2004) Nuclear magnetic resonance spectroscopy of high-molecular-weight proteins, *Annu. Rev. Biochem. 73*, 107−146.
44. Zhu, G., Xia, Y., Nicholson, L. K., and Sze, K. H. (2000) Protein dynamics measurements by TROSY-based NMR experiments, *J. Magn. Reson. 143*, 423−426.
45. Nilsson, J., Persson, B., and von Heijne, G. (2005) Comparative analysis of amino acid distributions in integral membrane proteins from 107 genomes, *Proteins 60*, 606−616.
46. Cornilescu, G., Delaglio, F., and Bax, A. (1999) Protein backbone angle restraints from searching a database for chemical shift and sequence homology, *J. Biomol. NMR 13*, 289−302.
47. Le, C. F., Bron, P., Verbavatz, J. M., Garret, A., Morel, G., Cavalier, A., Bonnec, G., Thomas, D., Gouranton, J., and Hubert, J. F. (1996) Incorporation of proteins into (*Xenopus*) oocytes by proteoliposome microinjection: Functional characterization of a novel aquaporin, *J. Cell Sci. 109* (Part 6), 1285−1295.
48. Marsal, J., Tigyi, G., and Miledi, R. (1995) Incorporation of acetylcholine receptors and Cl^- channels in *Xenopus* oocytes injected with *Torpedo electroplaque* membranes, *Proc. Natl. Acad. Sci. U.S.A. 92*, 5224−5228.
49. Miledi, R., Eusebi, F., Martinez-Torres, A., Palma, E., and Trettel, F. (2002) Expression of functional neurotransmitter receptors in *Xenopus* oocytes after injection of human brain membranes, *Proc. Natl. Acad. Sci. U.S.A. 99*, 13238−13242.
50. Mi, D., Kim, H. J., Hadziselimovic, A., and Sanders, C. R. (2006) Irreversible misfolding of diacylglycerol kinase is independent of aggregation and occurs prior to trimerization and membrane association, *Biochemistry 45*, 10072−10084.
51. Nagy, J. K., Kuhn, H. A., Keyes, M. H., Gray, D. N., Oxenoid, K., and Sanders, C. R. (2001) Use of amphipathic polymers to deliver a membrane protein to lipid bilayers, *FEBS Lett. 501*, 115−120.
52. Nagy, J. K., Lonzer, W. L., and Sanders, C. R. (2001) Kinetic study of folding and misfolding of diacylglycerol kinase in model membranes, *Biochemistry 40*, 8971−8980.
53. Popot, J. L., Berry, E. A., Charvolin, D., Creuzenet, C., Ebel, C., Engelman, D. M., Flotenmeyer, M., Giusti, F., Gohon, Y., Hong, Q., Lakey, J. H., Leonard, K., Shuman, H. A., Timmins, P., Warschawski, D. E., Zito, F., Zoonens, M., Pucci, B., and Tribet, C. (2003) Amphipols: Polymeric surfactants for membrane biology research, *Cell. Mol. Life Sci. 60*, 1559−1574.
54. Sanders, C. R., Kuhn, H. A., Gray, D. N., Keyes, M. H., and Ellis, C. D. (2004) French swimwear for membrane proteins, *ChemBioChem 5*, 423−426.
55. Gorzelle, B. M., Hoffman, A. K., Keyes, M. H., Gray, D. N., Ray, D. G., and Sanders, C. R. (2002) Amphipols can support the activity of a membrane enzyme, *J. Am. Chem. Soc. 124*, 11594−11595.
56. Pocanschi, C. L., Dahmane, T., Gohon, Y., Rappaport, F., Apell, H. J., Kleinschmidt, J. H., and Popot, J. L. (2006) Amphipathic polymers: Tools to fold integral membrane proteins to their active form, *Biochemistry 45*, 13954−13961.
57. Beyer, K., Leine, D., and Blume, A. (2006) The demicellization of alkyltrimethylammonium bromides in 0.1 M sodium chloride solution studied by isothermal titration calorimetry, *Colloids Surf., B 49*, 31−39.
58. Duchardt, E., Sigalov, A. B., Aivazian, D., Stern, L. J., and Schwalbe, H. (2007) Structure Induction of the T-Cell Receptor ζ-Chain upon Lipid Binding Investigated by NMR Spectroscopy, *ChemBioChem* (in press).
59. Klammt, C., Schwarz, D., Eifler, N., Engel, A., Piehler, J., Haase, W., Hahn, S., Dotsch, V., and Bernhard, F. (2007) Cell-free production of G protein-coupled receptors for functional and structural studies, *J. Struct. Biol.* (in press).
60. Krueger-Koplin, R. D., Sorgen, P. L., Krueger-Koplin, S. T., Rivera-Torres, I. O., Cahill, S. M., Hicks, D. B., Grinius, L., Krulwich, T. A., and Girvin, M. E. (2004) An evaluation of detergents for NMR structural studies of membrane proteins, *J. Biomol. NMR 28*, 43−57.
61. Tian, C., Breyer, R. M., Kim, H. J., Karra, M. D., Friedman, D. B., Karpay, A., and Sanders, C. R. (2005) Solution NMR spectroscopy of the human vasopressin V2 receptor, a G protein-coupled receptor, *J. Am. Chem. Soc. 127*, 8010−8011.
62. Tian, C., Breyer, R. M., Kim, H. J., Karra, M. D., Friedman, D. B., Karpay, A., and Sanders, C. R. (2005) Solution NMR spectroscopy of the human vasopressin v2 receptor, a G protein-coupled receptor, *J. Am. Chem. Soc. 127*, 8010−8011; (2006) *J. Am. Chem. Soc. 128*, 5300.
63. Aiyar, N., Nambi, P., Stassen, F., and Crooke, S. T. (1987) Solubilization and reconstitution of vasopressin V1 receptors of rat liver, *Mol. Pharmacol. 32*, 34−36.
64. Aiyar, N., Bennett, C. F., Nambi, P., Valinski, W., Angioli, M., Minnich, M., and Crooke, S. T. (1989) Solubilization of rat liver vasopressin receptors as a complex with a guanine-nucleotide-binding protein and phosphoinositide-specific phospholipase C, *Biochem. J. 261*, 63−70.
65. Aiyar, N., Valinski, W., Nambi, P., Minnich, M., Stassen, F. L., and Crooke, S. T. (1989) Solubilization of a guanine nucleotide-sensitive form of vasopressin V2 receptors from porcine kidney, *Arch. Biochem. Biophys. 268*, 698−706.

66. Huang, P., Liu, Q., and Scarborough, G. A. (1998) Lysophosphatidylglycerol: A novel effective detergent for solubilizing and purifying the cystic fibrosis transmembrane conductance regulator, *Anal. Biochem. 259*, 89−97.
67. Williams, K. A., Farrow, N. A., Deber, C. M., and Kay, L. E. (1996) Structure and dynamics of bacteriophage IKe major coat protein in MPG micelles by solution NMR, *Biochemistry 35*, 5145−5157.
68. Pervushin, K., Riek, R., Wider, G., and Wuthrich, K. (1997) Attenuated T2 relaxation by mutual cancellation of dipole-dipole coupling and chemical shift anisotropy indicates an avenue to NMR structures of very large biological macromolecules in solution, *Proc. Natl. Acad. Sci. U.S.A. 94*, 12366−12371.
69. Furukawa, T., Ono, Y., Tsuchiya, H., Katayama, Y., Bang, M. L., Labeit, D., Labeit, S., Inagaki, N., and Gregorio, C. C. (2001) Specific interaction of the potassium channel β-subunit minK with the sarcomeric protein T-cap suggests a T-tubule-myofibril linking system, *J. Mol. Biol. 313*, 775−784.
70. Chandrasekhar, K. D., Bas, T., and Kobertz, W. R. (2006) KCNE1 subunits require co-assembly with K^+ channels for efficient trafficking and cell surface expression, *J. Biol. Chem. 281*, 40015−40023.
71. Krumerman, A., Gao, X., Bian, J. S., Melman, Y. F., Kagan, A., and McDonald, T. V. (2004) An LQT mutant minK alters KvLQT1 trafficking, *Am. J. Physiol. 286*, C1453−C1463.

BI700705J